ACS OMEGA

http://pubs.acs.org/journal/acsodf

Article

Raman Spectroscopic and Quantum Chemical Investigation of the Pyridine-Borane Complex and the Effects of Dative Bonding on the Normal Modes of Pyridine

Ethan C. Lambert, Benjamin W. Stratton, and Nathan I. Hammer*

Cite This: *ACS Omega* 2022, 7, 13189−13195

Read Online

ACCESS | Metrics & More | Article Recommendations | Supporting Information

ABSTRACT: The pyridine-borane ($PyBH_3$) complex was analyzed by Raman vibrational spectroscopy and density functional theory to elucidate its structural and vibrational properties and to compare these with those for neat pyridine (Py). The borane−nitrogen (BN) bond length, the BN dative bond stretching frequency, and the effects of dative-bonded complex formation on Py are presented. Rather than having a single isolated stretching motion, the complex exhibits multiple BN dative bond stretches that are coupled to Py's vibrations. These modes exhibit large shifts that are higher in energy relative to neat Py, similar to previous observations of Py/water mixtures. However, significantly higher charge transfer was observed in the dative-bonded complex when compared to the hydrogen-bonded complex with water. A linear relationship between charge transfer and shifts to higher frequencies of pyridine's vibrational modes agrees well with earlier observations. The present work is of interest to those seeking a stronger relationship between charge-transfer events and concomitant changes in molecular properties.

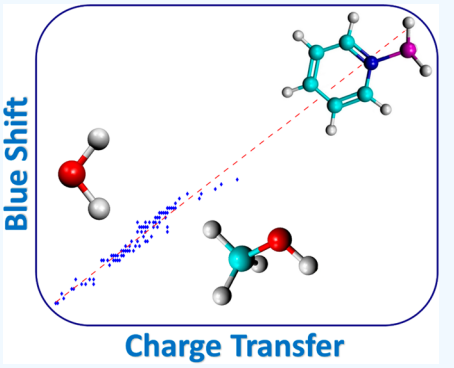

INTRODUCTION

A covalent bond typically involves a sharing of electrons between atoms, i.e., both atoms donate a single electron to be shared. A coordinate covalent or dative bond, however, forms from one atom donating a pair of electrons to a Lewis acid.[1−3] Boron's three valence electrons allow for the formation of three covalent bonds, with an empty p orbital remaining. This empty p orbital serves as a Lewis acid site and readily dative bonds to nitrogenous Lewis bases.[2,4] Dative bonds have been investigated both experimentally[5−9] and computationally[5−11] for the characterization of their vibrational frequencies, bond energies, and bond lengths. Vibrational frequencies vary because of substituent atoms, but the borane−nitrogen (BN) dative bond has a typical bond length of approximately 1.6 Å[8,9] and an interaction energy of −43.91 kcal mol^{-1} at the estimated CCSD(T) complete basis set limit.[11]

The vibrational frequencies of the BN dative bond stretching motion and dative-bonded complexes as a whole are of interest because of their potential to offer evidence of the significant charge transfer in dative bond formation. Shifts in vibrational energy have been studied extensively as a probe of intermolecular interactions.[12−19] In 2013,[19] we offered evidence of a strong correlation among charge transfer, vibrational mode shifts to higher energy, and changes in bond length in charge-donating, nitrogen-containing heterocycles. This work showed a linear relationship between the total electronic charge donated in a molecular complex and a shift to higher frequency in vibrational modes, particularly the ring breathing mode. Here, we extend our investigations of the effects of electron transfer in nitrogen-containing heterocycles to include the effects of dative bonding in the pyridine-borane complex. By characterizing the vibrations in this complex through Raman spectroscopy and comparing the spectrum to hydrogen-bonded complexes showing known charge-transfer events with pyridine,[16,17] a greater understanding of charge transfer in the dative bond, the correlation between charge transfer and changes in molecular properties, and the pyridine-borane complex can be obtained.

Since the development of its facile synthesis in 1954,[20] the pyridine-borane complex ($PyBH_3$) has been ubiquitous in molecular synthesis in roles such as a reducing agent,[21−26] a key component in reductive amination,[4,27−33] and a precursor to hydroborating alkenes at room temperature.[34−36] To the best of our knowledge, neither the Raman vibrational spectrum nor the BN dative bond stretch of $PyBH_3$ has been characterized. Borane−Lewis acid dative bonds have been studied extensively, as mentioned above, but pyridine (Py) has received little study as a Lewis base in dative bonds.[5,7] Matthäus et al. in 2001[7] studied boron trichloride-pyridine

Received: January 31, 2022
Accepted: March 25, 2022
Published: April 8, 2022

fragments and complexes through their pioneering vibrational fragment mode analysis technique. By describing vibrational modes in a complex as percentages of their fragment mode, they show mode mixing between Py and BCl_3 and large perturbations of the vibrational modes relative to their fragments. In 2003, Tao et al.[5] studied Py bound to Si(100) through vibrational spectroscopy and density functional theory (DFT) calculations to show that Py molecules interact with Si(100) through Si:N dative bonding. Tao et al. in 2008[6] published a similar work studying pyrrolidine dative bonds to Si(111)-7 × 7. Their work shows shifts to higher energy for pyrrolidine's ring breathing mode upon charge transfer and dative bond formation. The work by these groups lays a foundation for the study of the $PyBH_3$ dative-bonded complex in the present work.

Here, in an effort to investigate the vibrations of the $PyBH_3$ complex both in isolation and in comparison to Py and provide a greater correlation between charge transfer and vibrational mode shifts, we present a comprehensive Raman spectroscopic and DFT study. Raman spectra of Py and $PyBH_3$ are acquired experimentally and compared to explore the effects of the addition of BH_3 to Py's vibrational modes. These experimental results are also compared to Raman spectra of Py/water mixtures of various mole fractions, similar to the work of Schlucker et al.,[16] to compare the results of our work to a known charge-transfer event in Py. DFT calculations were performed to compare the structures of Py and $PyBH_3$, their simulated Raman spectra, and charge-transfer events through the natural electron configuration (NEC) within natural bond orbital (NBO) analyses. These calculations will show changes in bond length and aid in the characterization of $PyBH_3$'s Raman vibrational spectrum.

METHODS

Py (99.8%) and $PyBH_3$ (8 M BH_3Py) were commercially acquired from Sigma-Aldrich and used without further purification. All experimental data was acquired at ambient temperature using a Horiba LabRAM HR Evolution Raman Spectroscopy system (Horiba Scientific, Kyoto, Japan) equipped with a 600 grooves/mm grating and a charge-coupled device (CCD) detector. A 532 nm Nd:YAG laser (Oxxius, Lannion, France) was used to excite the solutions of Py, $PyBH_3$, and Py/water held in 1 cm cuvettes.

Calculations were carried out using the Gaussian 16 software suite.[37] Geometry optimizations (using the Opt = Very Tight option) and Raman activities were carried out using the Minnesota 06 functional M06-2X[38] with a correlation-consistent basis set augmented with diffuse functions (aug-cc-pVTZ).[39] This method and basis set will be denoted as M06-2X/aVTZ for the remainder of this work. To calculate the harmonic vibrational frequencies, a pruned numerical integration grid composed of 99 radial shells and 590 angular points per shell was employed, and these frequencies were scaled by an empirically determined scaling factor of 0.970 to partially account for anharmonicity and intermolecular interactions in condensed phases. Spectra were simulated by summing Lorentzian profiles constructed from the calculated harmonic frequencies and normalized Raman optical activities.

RESULTS AND DISCUSSION

Theoretical Predictions. Geometry optimizations and Raman vibrational frequency calculations of both Py and $PyBH_3$ were performed to compare and accurately characterize the vibrations of interest in the experimental data. Optimized structures of the $PyBH_3$ complex and Py are shown in Figure 1 with their associated bond lengths expressed in angstroms (Å) in Table 1. Cartesian coordinates for these molecules are available in the Supporting Information. The bond lengths here are reported to three decimal places to allow comparison; the precision is not intended to reflect the accuracy of the computed geometrical parameters. Upon formation of the $PyBH_3$ complex, NC1 and C5N bonds elongate by 0.006 Å (0.45%), the C2C3 and C3C4 bonds elongate by 0.001 Å (0.07%), and the C1C2 and C4C5 bonds shorten by 0.007 Å (0.50%). Steric hindrance could be present in the complex between the three boro-hydrogens and the neighboring pyridyl-hydrogens. This is relieved by the elongation of the NC1 and C5N bonds and the shortening of all CH bonds. The C1H8 and C5H11 bonds closest to the BH_3 group undergo shortenings greater in magnitude (0.004 Å, 0.37%) than those further removed (C2H9, C3H7, C4H10, 0.001 Å, 0.09%). We attribute the shortening of the C1C2 and C4C5 bonds to relieved ring strain in the stretched pyridine ring. The BN dative bond length is recorded as 1.615 Å and is in agreement with past works.[8,9] The BH14, BH13, and BH15 bonds are slightly longer than what has been recorded experimentally for BH_3 (1.190 Å)[40] and more closely agree with BH bond lengths for the boron dihydride anion (BH_2^-) or the boron hydride cation (BH^+), both with BH bond lengths of 1.205 Å.[40] The antiplanar BH bond, BH13, is slightly longer than its neighboring BH bonds, alluding to a more delocalized, weaker bond here.

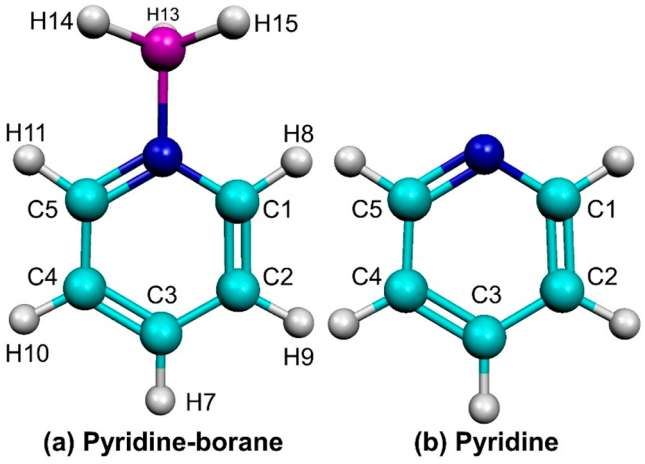

Figure 1. Optimized structures of $PyBH_3$ and Py at the M06-2X/aVTZ level of theory.

To provide a demonstrative quantification of charge transfer in the formation of the dative bond, natural electron configurations (NEC) were calculated for Py and BH_3 molecules each in isolation and in the $PyBH_3$ complex. These results are demonstrated in Table 2. To note, we do not present these data as a true value of charge transfer in the complex but rather as a relative quantification at the M06-2X level of theory. Charge transfer has been quantified with a wide range of theoretical methods,[41] and a variation in numeric value is expected. However, there should be no discrepancy between the methods in terms of the nature of the charge transferred, be it donation or receipt. The nitrogen atom

https://doi.org/10.1021/acsomega.2c00636
ACS Omega 2022, 7, 13189−13195

Table 1. Bond Lengths (R, Å) Associated with Py and $PyBH_3$ Structures Optimized at the M06-2X/aVTZ Level of Theory

molecule	R(N C1)[a]	R(C1 H8)	R(C1 C2)	R(C2 H9)	R(C2 C3)	R(C3 H7)	R(C3 C4)	R(C4 H10)	R(C4 C5)	R(C5 H11)	R(C5 N)	R(NB)	R(B H14)	R(B H13)	R(B H15)
pyridine	1.330	1.084	1.388	1.081	1.385	1.082	1.385	1.081	1.388	1.084	1.330	X	X	X	X
pyridine-borane	1.336	1.080	1.381	1.080	1.386	1.081	1.386	1.080	1.381	1.080	1.336	1.615	1.206	1.209	1.206
%Δ	0.45	0.37	0.50	0.09	0.07	0.09	0.07	0.09	0.50	0.37	0.45				

[a]See Figure 1 for atom numbers. Data given to three decimal places to facilitate comparison.

experiences a large decrease in natural electron population as the complex forms. This is correlated with a decrease in the populations of carbons 1, 3, and 5 as well. Carbons 1 and 5 are closest to the dative bond and undergo a larger magnitude of charge transfer than carbon 3. Interestingly, carbons 2 and 4 are unperturbed within the precision of our calculations. Hydrogens 8 and 11, those proximal to the nitrogen atom, undergo a relatively large depletion of natural population as the dative-bond formation draws charge from the ring structure. Hydrogens 7, 9, and 10 are still seen to lose charge in the $PyBH_3$ complex but to a smaller degree than do the other pyridyl hydrogens. The borohydrogens, hydrogen 13, 14, and 15, also are depleted of electronic population in the dative-bonded complex, with the highest depletion in antiplanar hydrogen 13. The depletion of charge in the Py molecule is coupled with the large increase in the natural population of the boron atom upon complex formation. This charge transfer is consistent with established BN dative-bond formation and should correlate with shifts in the Raman spectra of Py upon complex formation.

Table 2. Charge Transfer (me^-) Associated with the Py Atoms after the Formation of the Dative Bond in $PyBH_3$

atom[a]		Δq (me^-)
C	1	−50
C	2	0
C	3	−30
C	4	0
C	5	−50
N	6	−50
H	7	−10
H	8	−40
H	9	−10
H	10	−10
H	11	−40
B	12	530
H	13	−80
H	14	−60
H	15	−60

[a]See Figure 1 for atom numbers.

Simulated Raman spectra of both Py (bottom, black) and $PyBH_3$ (top, green) at the M06-2X/aVTZ level of theory are shown in Figure 2, with tabulated spectral shifts recorded in Table 3. Full simulated spectra are available in the Supporting Information. Predicted spectral shifts are demonstrated with red arrows. Mode assignments for Py are based upon work by Wilmshurst and Bernstein[42] and were employed to assign the modes in $PyBH_3$. In the simulated spectrum of $PyBH_3$, the BN dative-bond stretch appears at two separate energies, both coupled to a pyridine vibration. The first appears at 695 cm^{-1} and is coupled to pyridine's ν_{6a} vibrational mode. This mode is

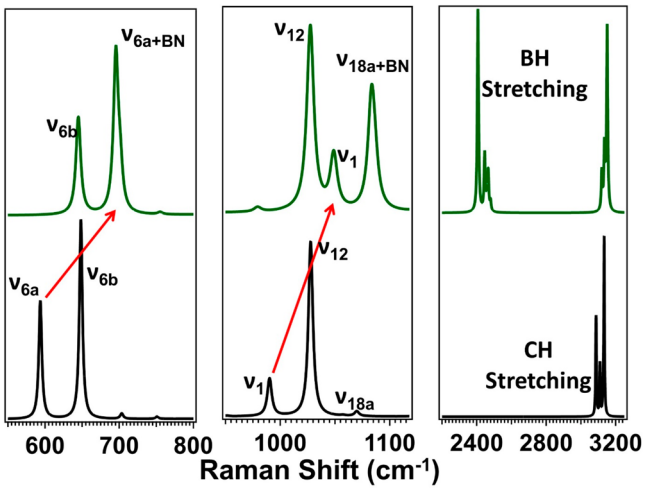

Figure 2. Simulated Raman spectra of Py (black, bottom) and $PyBH_3$ (green, top) at the M06-2X/aVTZ level of theory. Red arrows denote large shifts in the Raman spectra.

Table 3. Spectral Shifts Associated with Py and $PyBH_3$ Simulated Raman Spectra (Figure 2)[a]

mode	Py (cm^{-1})	$PyBH_3$ (cm^{-1})	$\Delta\nu$ (cm^{-1})
ν_1	990	1049	59
ν_{6a}	594	695	101
ν_{6b}	648	645	−3
ν_{12}	1028	1028	0
ν_{18a}	1070	1083	13

[a]The computed energies have been scaled by 0.97.

predicted to occur in neat pyridine at 594 cm^{-1} and involves a symmetric stretching and contracting of the NC1−C5N and C2C3−C3C4 bonds. The +101 cm^{-1} shift seen upon formation of the $PyBH_3$ complex is correlated with these changes in bond lengths and charge transfer, perturbing the vibrational frequency. The second BN dative-bond stretch is predicted to occur at 1083 cm^{-1}, coupled to pyridine's ν_{18a} vibrational mode. Neat Py's ν_{18a} vibrational mode is predicted to occur at 1070 cm^{-1}. This vibration features a shift to higher energy relative to neat Py, correlated with the stretching motions by the elongated NC1−C5N and C2C3−C3C4 bonds.

In Py's simulated Raman spectrum, the ν_{18a} vibrational mode is relatively weak compared to the Raman activities of the adjacent vibrations. In the $PyBH_3$ simulated spectrum, ν_{18a} has undergone a large increase in Raman activity relative to its adjacent modes, indicating an increase in proportion to this vibration.

The ν_{6b} vibration is predicted to be relatively unperturbed, shifting from 648 cm^{-1} in Py to 645 cm^{-1} in $PyBH_3$. This small shift to lower frequency is attributed to an overall lack of bond

https://doi.org/10.1021/acsomega.2c00636
ACS Omega 2022, 7, 13189−13195

stretching and compression in this vibrational mode. A similar phenomenon is seen with the ν_{12} mode, predicted to occur at 1028 cm^{-1} in both Py and $PyBH_3$. The ν_{12} vibrational mode is sometimes denoted as a triangle mode and is similar in motion to a ring breathing mode. This mode features a symmetric radial contraction and expansion of C1, C3, and C5. Neither vibrational mode mentioned involves any vibration of the nitrogen atom or the BN dative bond, which correlates with their small predicted shift. There is a small peak observed at 703 cm^{-1} in the simulated spectrum of isolated pyridine. This mode is an out-of-plane symmetric C−H wagging motion and is present at 690 cm^{-1} in the $PyBH_3$ spectrum but is unresolved because of the breadth of the ν_{6a} peak.

As mentioned above, the ring breathing mode (ν_1) has long been a probe of interactions in the azabenzenes. This mode, not unlike the triangle mode, involves a symmetrical radial contraction and expansion of N, C2, and C4. Py's ν_1 mode is predicted to occur at 990 cm^{-1} and undergo a large shift higher in frequency to 1049 cm^{-1} in $PyBH_3$. Similar to the vibrations discussed above, it involves a vibration of the nitrogen atom/BN dative bond and is significantly shifted to higher frequency. Theory also predicts a slight shift higher in frequency of the CH stretching modes (approximately 3100 cm^{-1}) in $PyBH_3$ relative to neat Py. This change in vibrational frequency is correlated with a shortening and stiffening of the CH bonds upon complex formation.

A 2013 study[19] performed by our group examined shifts in vibrational frequency as a function of total electronic charge transferred by a nitrogen-containing heterocycle in complex with several Lewis acid solvents. These earlier results showed a linear relationship between charge transfer and spectral shift, which was strongest with the ν_1 ring breathing mode and had an R^2 value of 0.952 for >100 unique microsolvated structures. Interestingly, taking the total computed charge transfer into account (Table 2, 180 me^-), the computationally predicted shift in ν_1 in nitrogen-containing heterocycles using our previously reported results is about 60 cm^{-1}, in excellent agreement with the computed prediction in Table 3. This result simultaneously strengthens the evidence for the charge-transfer event in the $PyBH_3$ dative-bond formation and the correlation between charge transfer and shifts to higher vibrational frequency in nitrogen heterocyclic complexes.

Experimental Results. *Mode Assignments.* Characterization of the simulated Raman spectrum of $PyBH_3$ allows for the assignment of vibrational modes in the experimental spectrum. The simulated Raman spectrum of $PyBH_3$ at the M06-2X/aVTZ level of theory is compared to experimental data for $PyBH_3$ in Figure 3. Full spectra are available in the Supporting Information. Table 4 contains the locations of the assigned modes of interest. A low activity peak is present at approximately 990 cm^{-1} experimentally, corresponding to a peak at 979 cm^{-1} in the simulated spectrum. Because of its wavenumber location, this peak could be assumed to be ν_1; however, an analysis of the vibration reveals it to be a BN rocking motion. The ν_1 mode is assigned to an ill-resolved shoulder of the ν_{12} peak at approximately 1032 cm^{-1} in the experimental data. Figure S3 compares an experimental Raman spectrum of $PyBH_3$ to a less-resolved simulated spectrum. This simulated spectrum was obtained by increasing the Lorentzian fwhm of the vibrational modes. This comparison better shows the similarity between the simulated and experimental data for the ν_1 mode in $PyBH_3$ and offers strong evidence for its location as a shoulder of the ν_{12} mode. A peak is present at approximately 610 cm^{-1} in the experimental data that does not appear in the simulated data. Because this feature is present in neat pyridine (Figure 4), we believe that this mode may be a result of some dissociated Py in $PyBH_3$. The BH stretching region (approximately 2400 cm^{-1}) is less resolved, with a larger fwhm for each peak. Although this could stem from rovibrational populations within the sample, a more likely explanation is contributions from boron's two isotopes. The breadth of this region can be replicated in simulated Raman spectra, not unlike what is demonstrated in Figure S3.

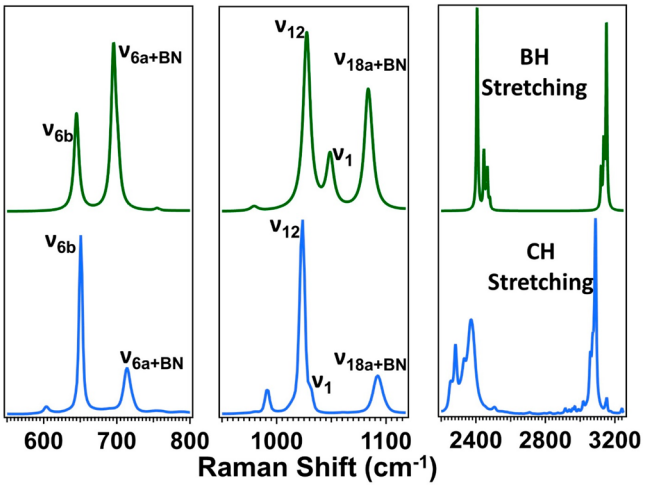

Figure 3. Simulated Raman spectra of $PyBH_3$ (top, green) at the M06-2X/aVTZ level of theory compared to experimental data for the same complex (bottom, blue).

Table 4. Predicted (M06-2X/aVTZ) and Experimental Locations of the Vibrational Modes of Interest in $PyBH_3$[a]

mode	theory (cm^{-1})	experiment (cm^{-1})
ν_1	1049	1032
ν_{6a}	695	714
ν_{6b}	645	651
ν_{12}	1028	1024
ν_{18a}	1083	1093

[a]The computed energies have been scaled by 0.97.

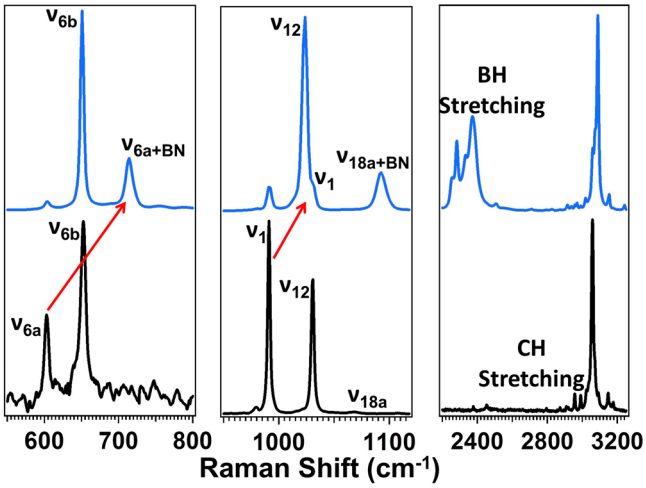

Figure 4. Experimental Raman spectra of Py (bottom, black) and $PyBH_3$ (top, blue). Red arrows denote large shifts in the Raman spectra.

https://doi.org/10.1021/acsomega.2c00636
ACS Omega 2022, 7, 13189−13195

Comparison to Neat Pyridine. The assignment of vibrational modes in $PyBH_3$'s Raman spectrum allows for comparison to neat Py's Raman spectrum in order to track shifts in Py's peaks as a function of complex formation. Experimental Raman spectra for Py (bottom, black) and $PyBH_3$ (top, blue) are compared in Figure 4. Full experimental spectra are available in the Supporting Information. The results for selected modes of interest are recorded in Table 4. In agreement with theory, both ν_1 and ν_{6a} shift higher in energy upon complex formation, shifting higher in energy than ν_{12} and ν_{6b}, respectively. Vibrations ν_{6b} and ν_{12} undergo small wavenumber shifts to lower energy, and ν_{18a} undergoes a shift to higher energy and an increase in intensity relative to ν_1 and ν_{12}, also in agreement with theory. The CH stretching region shifts slightly higher in energy, as predicted.

Comparison to Pyridine/Water Clusters. Past studies[12,19] have connected charge transfer in nitrogen-containing heterocycles to shifts to higher energy in vibrational modes, particularly ν_1. When forming the dative bond, both of the pyridyl-nitrogen's lone pairs are donated to the boron atom's empty orbital. This charge transfer is large in magnitude and should result in a shift to a higher energy of ν_1 that is larger in magnitude than that resulting from a smaller charge transfer. This effect is demonstrated by comparing the results obtained here to spectral shifts observed in Py−water hydrogen-bonded networks, similar to work performed by Schlucker et al.[16] The experimental shifts of the above studied modes and the CH stretching region due to hydrogen bonding with increasing mole fractions of water are compared with those in the $PyBH_3$ complex in Figure 5. Shifts for the characterized vibrational modes are recorded in Table 5. Full experimental spectra are available in the Supporting Information.

At the lowest mole fraction ratio of pyridine/water, the majority of the Py molecules are participating with surrounding water molecules through N···H−O hydrogen bonding, resulting in a shift in ν_1 by +10 cm^{-1}. When this shift is compared to the experimental $PyBH_3$-induced shift of +41 cm^{-1}, it can be predicted that a much larger amount of charge is transferred during dative-bond formation, in agreement with the results shown in Table 1. The ν_{6a} vibrational mode serves as another probe of charge transfer in the hydrogen-bonded species, shifting by +12 cm^{-1}; ν_{18a} is also minutely affected by

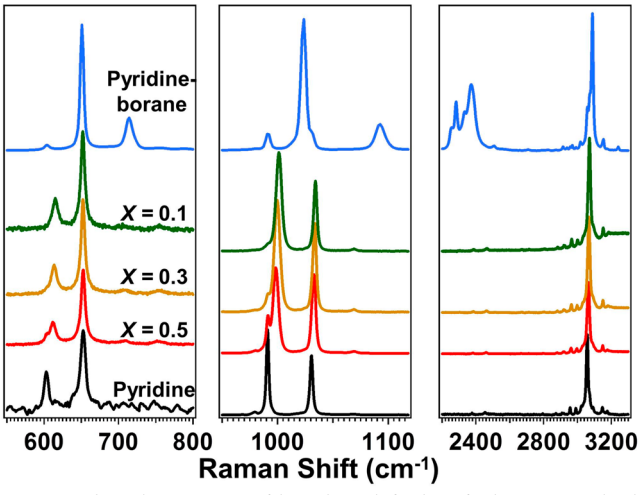

Figure 5. Experimental Raman spectra of decreasing mole fractions of Py/water compared to the $PyBH_3$ complex.

Table 5. Spectral Shifts Induced in Py by Hydrogen Bonding and $PyBH_3$ Complex Formation

mode	Py	$PyBH_3$	$\Delta\nu$ $PyBH_3$	X = 0.1 Py/water	$\Delta\nu$ X = 0.1 Py/water
ν_1	991	1032	41	1001	10
ν_{6a}	603	714	111	615	12
ν_{6b}	652	651	−1	652	0
ν_{12}	1031	1024	−7	1034	3
ν_{18a}	1068	1093	25	1069	1

the introduction of water, compared to a large change in energy and activity in the $PyBH_3$ complex. The coupling of BN stretching motions to ν_1, ν_{6a}, and ν_{18b} in the $PyBH_3$ complex is further linked to the large shifts in the Raman spectrum of Py. In the Py-water complexes, ν_{12} and ν_{6b} are relatively unaffected, indicating a comparable degree of perturbation of energy to the $PyBH_3$ complex. The CH stretching region as a whole also consistently shifts higher in energy upon charge transfer, with the highest shift occurring for the $PyBH_3$ complex. The results here offer strong evidence of the significant amount of charge transferred during $PyBH_3$ complex formation relative to that for hydrogen-bonded complexes. They also strengthen the conclusions stated previously correlating blue shifts with the charge transfer of vibrational modes.[19]

CONCLUSIONS

The Raman vibrational spectrum and charge-transfer properties of the pyridine-borane ($PyBH_3$) complex are demonstrated in relation to neat pyridine by Raman vibrational spectroscopy and density functional theory (M06-2X/aug-cc-pVTZ method and basis set). This complex is found to have a length of 1.615 Å and two stretching frequencies coupled to pyridine's vibrational modes at 714 and 1093 cm^{-1}. A significant amount of electronic charge is transferred from the pyridine (Py) molecule upon dative-bonded complex formation. This charge transfer is correlated with a shift in the ring breathing mode of Py to higher vibrational frequency. This finding is in strong agreement with our past study which shows a linear relationship between charge transfer and spectral shifts to higher energy. Upon complex formation, there are also changes in bond length to relieve both steric hindrance and ring strain. Experimental shifts in vibrational modes for the $PyBH_3$ complex were compared to shifts acquired for Py-water hydrogen-bonded complexes, which have been previously correlated to charge transfer. Larger vibrational frequency shifts were seen in the dative-bonded complex than in hydrogen-bonded complexes, indicating a higher degree of transferred electronic charge. The work employs DFT to demonstrate charge-transfer events in dative bond formation and is of interest to those attempting to characterize the physical properties of molecular complexes.

ASSOCIATED CONTENT

Supporting Information

The Supporting Information is available free of charge at https://pubs.acs.org/doi/10.1021/acsomega.2c00636.

Full Raman spectra of all figures and Cartesian coordinates of optimized molecular structures (PDF)

https://doi.org/10.1021/acsomega.2c00636
ACS Omega 2022, 7, 13189−13195

AUTHOR INFORMATION

Corresponding Author

Nathan I. Hammer − *Department of Chemistry and Biochemistry, University of Mississippi, University, Mississippi 38655, United States;* orcid.org/0000-0002-6221-2709; Phone: 662-915-3989; Email: nhammer@olemiss.edu

Authors

Ethan C. Lambert − *Department of Chemistry and Biochemistry, University of Mississippi, University, Mississippi 38655, United States*

Benjamin W. Stratton − *Department of Chemistry and Biochemistry, University of Mississippi, University, Mississippi 38655, United States;* Present Address: Department of Chemistry, University of Georgia, Athens, Georgia 30602, United States

Complete contact information is available at: https://pubs.acs.org/10.1021/acsomega.2c00636

Funding

This article has been supported by the National Science Foundation (OIA-1757220 and CHE-1532079) and the Sally McDonnell Barksdale Honors College at the University of Mississippi. The computations in this article were performed using resources at the Mississippi Center for Supercomputing Resources (MCSR).

Notes

The authors declare no competing financial interest.

ABBREVIATIONS

aVTZ, aug-cc-pVTZ; BN, borane−nitrogen; DFT, density functional theory; NBO, natural bond orbital; NEC, natural electron configuration; Py, pyridine; $PyBH_3$, pyridine-borane complex; aVTZ, aug-cc-pVTZ;

REFERENCES

(1) Pupim, C. F.; Catão, A. J. L.; López-Castillo, A. Boron−nitrogen dative bond. *J. Mol. Model.* **2018**, *24* (10), 283.

(2) Frenking, G. Peculiar boron startles again. *Nature* **2015**, *522* (7556), 297−298.

(3) Nandi, A.; Kozuch, S. History and Future of Dative Bonds. *Chemistry − A European Journal* **2020**, *26* (4), 759−772.

(4) Molander, G. A.; Cooper, D. J. Functionalization of organotrifluoroborates: Reductive amination. *J. Org. Chem.* **2008**, *73* (10), 3885−3891.

(5) Tao, F.; Qiao, M. H.; Wang, Z. H.; Xu, G. Q. Dative and Di−σ Binding States of Pyridine on Si(100) and Their Thermal Stability. *J. Phys. Chem. B* **2003**, *107* (26), 6384−6390.

(6) Tao, F.; Cai, Y.; Ning, Y.; Xu, G.-Q.; Bernasek, S. L. Transfer of Electron Density and Formation of Dative Bonds in Chemisorption of Pyrrolidine on Si(111)-7 × 7. *J. Phys. Chem. C* **2008**, *112* (39), 15474−15482.

(7) Matthäus, C.; Wheeler, R. A. Fragment mode analysis and its application to the vibrational normal modes of boron trichloride−ammonia and boron trichloride−pyridine complexes. *Spectrochim. Acta, Part A* **2001**, *57* (3), 521−534.

(8) Dreux, K. M.; McNamara, L. E.; Kelly, J. T.; Wright, A. M.; Hammer, N. I.; Tschumper, G. S. Probing Dative and Dihydrogen Bonding in Ammonia Borane with Electronic Structure Computations and Raman under Nitrogen Spectroscopy. *J. Phys. Chem. A* **2017**, *121* (31), 5884−5893.

(9) Reinemann, D. N.; Wright, A. M.; Wolfe, J. D.; Tschumper, G. S.; Hammer, N. I. Vibrational Spectroscopy of N-Methyliminodiacetic Acid (MIDA)-Protected Boronate Ester: Examination of the B−N Dative Bond. *J. Phys. Chem. A* **2011**, *115* (24), 6426−6431.

(10) De Silva, C. C.; Holme, T. A. Computational studies of dative bond containing heterocyclic ring structures. *Comput. Theor. Chem.* **2013**, *1019*, 78−84.

(11) Karthikeyan, S.; Sedlak, R.; Hobza, P. on the Nature of Stabilization in Weak, Medium, and Strong Charge-Transfer Complexes: CCSD(T)/CBS and SAPT Calculations. *J. Phys. Chem. A* **2011**, *115* (34), 9422−9428.

(12) Howard, A. A.; Tschumper, G. S.; Hammer, N. I. Effects of hydrogen bonding on vibrational normal modes of pyrimidine. *J. Phys. Chem. A* **2010**, *114* (25), 6803−6810.

(13) Howard, J. C.; Hammer, N. I.; Tschumper, G. S. Structures, energetics and vibrational frequency shifts of hydrated pyrimidine. *ChemPhysChem* **2011**, *12* (17), 3262−3273.

(14) Cabaco, M. I.; Besnard, M.; Yarwood, J. Raman spectroscopic studies of vibrational relaxation and chemical exchange broadening in hydrogen bonded systems. I. Investigation of relaxation processes in binary mixtures of pyridine and ethanol. *Mol. Phys.* **1992**, *75* (1), 139−155.

(15) Schlücker, S.; Koster, J.; Singh, R. K.; Asthana, B. P. Hydrogen-bonding between pyrimidine and water: A vibrational spectroscopic analysis. *J. Phys. Chem. A* **2007**, *111* (24), 5185−5191.

(16) Schlücker, S.; Singh, R. K.; Asthana, B. P.; Popp, J.; Kiefer, W. Hydrogen-bonded pyridine-water complexes studied by density functional theory and raman spectroscopy. *J. Phys. Chem. A* **2001**, *105* (43), 9983−9989.

(17) Takahashi, H.; Mamola, K.; Plyler, E. K. Effects of hydrogen bond formation on vibrations of pyridine, pyrazine, pyrimidine, and pyridazine. *J. Mol. Spectrosc.* **1966**, *21* (1−4), 217−230.

(18) Zoidis, E.; Yarwood, J.; Danten, Y.; Besnard, M. Spectroscopic studies of vibrational relaxation and chemical exchange broadening in hydrogen-bonded systems. III. Equilibrium processes in the pyridine/water system. *Mol. Phys.* **1995**, *85* (2), 373−383.

(19) Wright, A. M.; Howard, A. A.; Howard, J. C.; Tschumper, G. S.; Hammer, N. I. Charge Transfer and Blue Shifting of Vibrational Frequencies in a Hydrogen Bond Acceptor. *J. Phys. Chem. A* **2013**, *117* (26), 5435−5446.

(20) Taylor, M. D.; Grant, L. R.; Sands, C. A. A Convenient Preparation of Pyridine-Borane. *J. Am. Chem. Soc.* **1955**, *77* (6), 1506−1507.

(21) Ambrogelly, A.; Cutler, C.; Paporello, B. Screening of reducing agents for the pegylation of recombinant human IL-10. *Protein Journal* **2013**, *32* (5), 337−342.

(22) Gurram, S.; Srivastava, G.; Badve, V.; Nandre, V.; Gundu, S.; Doshi, P. Pyridine Borane as Alternative Reducing Agent to Sodium Cyanoborohydride for the PEGylation of L-asparaginase. *Appl. Biochem. Biotechnol.* **2022**, *194*, 827.

(23) Kawase, M.; Kikugawa, Y. Chemistry of amine-boranes. Part 5. Reduction of oximes, O-acyl-oximes, and O-alkyl-oximes with pyridine-borane in acid. *J. Chem. Soc., Perkin Trans. 1* **1979**, 643−645.

(24) Kikugawa, Y.; Saito, K.; Yamada, S. I. Reduction of heterocycles with pyridine: Borane in acetic acid. *Synthesis (Germany)* **1978**, *1978* (6), 447−448.

(25) Matsuoka, M.; Hayashi, T. Chemical Nickel plating using pyridine borane as a reducing agent. *Plat. Surf. Finish.* **1981**, *68* (7), 66−69.

(26) Wong, W. S. D.; Osuga, D. T.; Feeney, R. E. Pyridine borane as a reducing agent for proteins. *Anal. Biochem.* **1984**, *139* (1), 58−67.

(27) Abdel-Magid, A. F.; Carson, K. G.; Harris, B. D.; Maryanoff, C. A.; Shah, R. D. Reductive amination of aldehydes and ketones with sodium triacetoxyborohydride. Studies on direct and indirect reductive amination procedures. *J. Org. Chem.* **1996**, *61* (11), 3849−3862.

(28) Bomann, M. D.; Guch, I. C.; DiMare, M. A Mild, Pyridine-Borane-Based Reductive Animation Protocol. *J. Org. Chem.* **1995**, *60* (18), 5995−5996.

(29) Khanna, I. K.; Weier, R. M.; Lentz, K. T.; Swenton, L.; Lankin, D. C. Facile, Regioselective Syntheses of N-Alkylated 2, 3-Diaminopyridines and Imidazo[4, 5-b]pyridines. *J. Org. Chem.* **1995**, *60* (4), 960−965.

(30) Krusemark, C. J.; Ferguson, J. T.; Wenger, C. D.; Kelleher, N. L.; Belshaw, P. J. Global amine and acid functional group modification of proteins. *Anal. Chem.* **2008**, *80* (3), 713−720.
(31) Moormann, A. E. Reductive amination of piperidines with aldehydes using borane-pyridine. *Synth. Commun.* **1993**, *23* (6), 789−795.
(32) Pelter, A.; Rosser, R. M.; Mills, S. Reductive aminations of ketones and aldehydes using borane-pyridine. *J. Chem. Soc., Perkin Trans. 1* **1984**, 717−720.
(33) Stults, N. L.; Asta, L. M.; Lee, Y. C. Immobilization of proteins on oxidized crosslinked sepharose preparations by reductive amination. *Anal. Biochem.* **1989**, *180* (1), 114−119.
(34) Brown, H. C.; Vara Prasad, J. V. N.; Zee, S. H. Hydroboration. 75. Directive Effects in the Hydroboration of Vinyl and Propenyl Heterocycles with Representative Hydroborating Agents. *J. Org. Chem.* **1986**, *51* (4), 439−445.
(35) Clay, J. M.; Karatjas, A. G.; Vedejs, E. Hydroboration with pyridine borane at room temperature. *J. Am. Chem. Soc.* **2008**, *130* (32), 10828.
(36) Clay, J. M.; Vedejs, E. Hydroboration with pyridine borane at room temperature. *J. Am. Chem. Soc.* **2005**, *127* (16), 5766−5767.
(37) Frisch, M. J., et al. *Gaussian 16*, Revision C.01; Gaussian, Inc.: Wallingford, CT, 2016
(38) Zhao, Y.; Truhlar, D. G. The M06 suite of density functionals for main group thermochemistry, thermochemical kinetics, noncovalent interactions, excited states, and transition elements: two new functionals and systematic testing of four M06-class functionals and 12 other functionals. *Theor. Chem. Acc.* **2008**, *120* (1), 215−241.
(39) Dunning, T. H. Gaussian basis sets for use in correlated molecular calculations. I. The atoms boron through neon and hydrogen. *J. Chem. Phys.* **1989**, *90* (2), 1007−1023.
(40) Kuchitsu, K. Inorganic molecules. In *Structure of Free Polyatomic Molecules: Basic Data*; Kuchitsu, K., Ed.; Springer: Berlin, 1998; pp 25−78.
(41) Weinhold, F.; Landis, C. R.; Glendening, E. D. What is NBO analysis and how is it useful? *Int. Rev. Phys. Chem.* **2016**, *35* (3), 399−440.
(42) Wilmshurst, J. K.; Bernstein, H. J. the Vibrational Spectra of Pyridine, Pyridine-4-d, Pyridine-2,6-d2, and Pyridine-3,5-d2. *Can. J. Chem.* **1957**, *35* (10), 1183−1194.

https://doi.org/10.1021/acsomega.2c00636
ACS Omega 2022, 7, 13189−13195